View metadata, citation and similar papers at core.ac.uk

brought to you by CORE

provided by IR@CECRI

Journal of The Electrochemical Society, **155** (3) A206-A210 (2008)
0013-4651/2008/155(3)/A206/5/$23.00 © The Electrochemical Society

Sol-Gel Synthesis of 5 V $LiCu_xMn_{2-x}O_4$ as a Cathode Material for Lithium Rechargeable Batteries

A. Sulochana,[a] R. Thirunakaran,[a] A. Sivashanmugam,[a] S. Gopukumar,[a,z] and Jun-ichi Yamaki[b,*]

[a]*Central Electrochemical Research Institute, Karaikudi-630 006, Tamil Nadu, India*
[b]*Institute of Advanced Materials Chemistry and Engineering, Kyushu University, Kasuga 816-8580, Japan*

Spinel $LiCu_xMn_{2-x}O_4$ ($0.025 \leq x \leq 0.1$) has been synthesized using oxalic acid as the chelating agent using a sol-gel method to obtain submicrometer-sized particles, good surface morphology, homogeneity, agglomeration, and high crystallinity involving short heating time. X-ray diffraction (XRD), scanning electron microscopy (SEM), Fourier transform infrared spectroscopy, and thermogravimetric and differential thermal analysis were carried out for the physical characterization of the synthesized powder. The XRD patterns of $LiCu_xMn_{2-x}O_4$ show the single-phase spinel product, which is in good agreement with the JCPDS card (35-782). SEM images show that the particles, on the average, are of 50 nm in size and are present as agglomerated clusters at all dopant levels. Electrochemical cycling studies of the compound were carried out between 3 and 5 V to understand the redox behavior of Cu^{2+} ions. The charge–discharge cycling studies of spinel material with Cu stoichiometry of $x = 0.1$ calcined at 850°C exhibit an initial discharge capacity of 130 mAh g^{-1} and stabilized at 120 mAh g^{-1}.
© 2008 The Electrochemical Society. [DOI: 10.1149/1.2828030] All rights reserved.

Manuscript submitted October 5, 2007; revised manuscript received November 28, 2007. Available electronically January 8, 2008.

$LiMn_2O_4$ spinel is an attractive cathode material for lithium rechargeable batteries due to its low cost, easy availability, and low toxicity when compared to other layered positive cathode materials, such as $LiNiO_2$ and $LiCoO_2$.[1-4] Despite satisfactory cycling behavior of $LiMn_2O_4$ at room temperature, capacity fading occurs when cycled at high voltage and elevated temperatures.[5,6] Material scientists employ several monovalent, divalent, trivalent, tetravalent, and pentavalent cations (Li^+, Fe^{2+}, Ni^{2+}, Co^{2+}, Al^{3+}, Cr^{3+}, Ti^{4+}, V^{5+}, etc.) as dopants for substituting manganese ions to derive better electrochemical activity without capacity fade upon cycling.[7] Furthermore, the capacity fade is attributed to several factors viz. oxygen deficiency,[5] Jahn–Teller distortion,[8] lattice instability,[9] particle disruption,[10] slow dissolution of $LiMn_2O_4$,[11] etc., and such materials have been charged above 4.5 V. In order to obtain submicrometer-sized particles of $LiMn_2O_4$, several soft chemistry methods, such as oxalic acid–assisted sol-gel synthesis,[12-17] precipitation,[18] the pechini process,[19] and the hydrothermal method,[20] have been employed by several researchers. In this present work, spinel $LiCu_xMn_{2-x}O_4$ has been synthesized using oxalic acid as the chelating agent in which manganese was partially substituted by transition metal copper to stabilize the capacity fade up to 15 cycles.

Experimental

Figure 1 shows the schematic flow sheet of the synthesis procedure for $LiCu_xMn_{2-x}O_4$ using oxalic acid as the chelating agent by a sol-gel route with Cu doping in the range of $0.025 \leq x \leq 0.1$. Stoichiometric amounts of lithium nitrate (E. Merck), manganese nitrate (E. Merck), and copper nitrate (Glaxo) were uniformly mixed and dissolved in deionized water. This solution was stirred continuously with mild heating, and oxalic acid (E. Merck) was also added simultaneously to get a homogeneous solution of $LiCu_xMn_{2-x}O_4$. The pH of the solution was adjusted between 7 and 8.5. This process of stirring and heating was continued until a solid gel was obtained. Furthermore, the gel was initially heated at 110°C overnight. The thermal behavior of the precursors was characterized by thermogravimetric and differential thermal analysis (TG/DTA) (PL Thermal Sciences Instrument, model STA 1500). The experiments were carried out in air at a heating ramp of 20°C/min with typically 50 mg samples. Furthermore, this gel mass was calcined at different temperatures viz., 250, 400, 600, and 850°C for 4 h in alumina crucibles. The resulting calcined samples were subjected to XRD [JEOL 8030 X-ray diffraction (XRD) with nickel filtered Cu Kα radiation], SEM (Hitachi S-3000 H), transmission electron microscopy [(TEM), FEI-Tecnai-20 G2], and Fourier transform infrared spectroscopy [(FTIR), Perkin-Elmer, model Paragon-500 spectrophotometer] studies for physical characterization.

Electrochemical cell assembly.— The electrochemical cell was a typical 2016 coin cell (Hohsen Co., Japan) assembled using lithium metal as the anode, Celgard 2400 as the separator, and 1 M solution of $LiPF_6$ in a 3:7 (V/V) mixture of ethylene carbonate/methyl ethyl carbonate as electrolyte and $LiCu_xMn_{2-x}O_4$ as cathode active material. The cathodes were prepared by slurry coating over an aluminum foil of 18 mm diam. The slurry is an 80:10:10 mixture of cathode active material, acetylene black, and poly(vinylidene fluoride) in *n*-methyl-2-pyrrolidone. The loading of active material in the cathode varied from 0.087 to 0.098 g. Charge–discharge studies were carried out between 3.0 and 5.0 V at a C/10 rate.

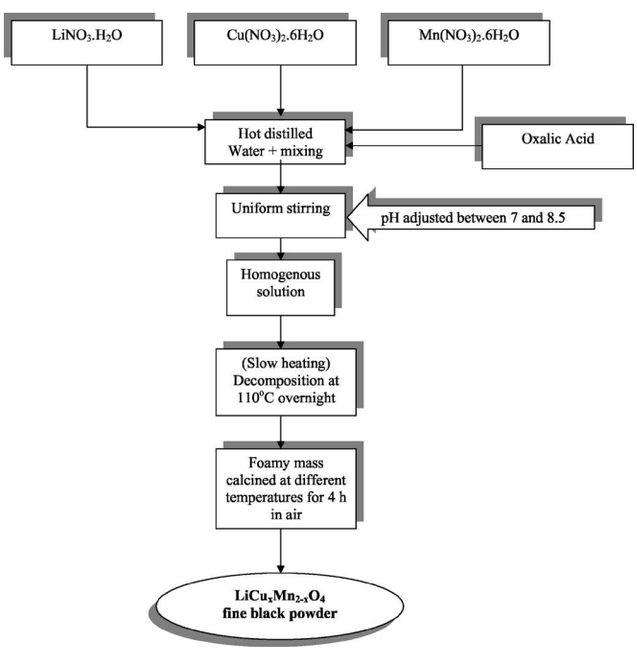

Figure 1. Flow chart for the synthesis of $LiCu_xMn_{2-x}O_4$ by a sol-gel route using oxalic acid as the chelating agent.

* Electrochemical Society Active Member.
z E-mail: deepika_41@rediffmail.com

Downloaded 13 Feb 2009 to 210.212.252.226. Redistribution subject to ECS license or copyright; see http://www.ecsdl.org/terms_use.jsp

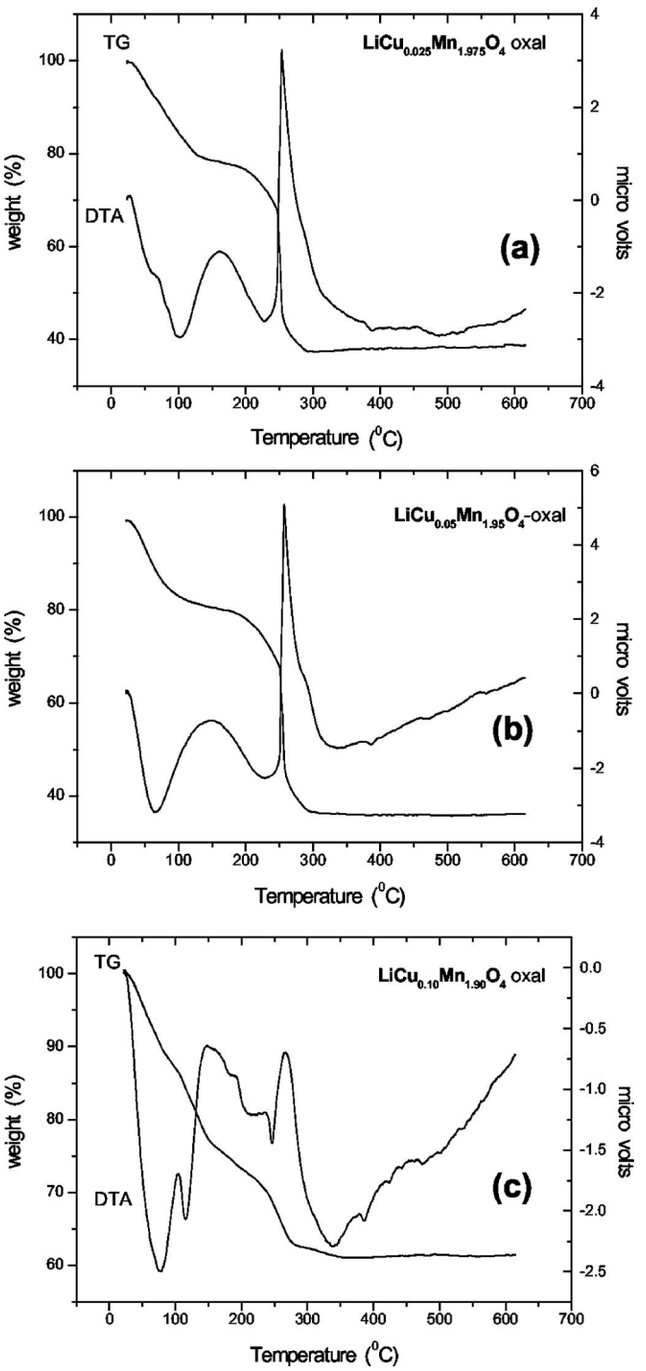

Figure 2. TG/DTA curves of $LiCu_xMn_{2-x}O_4$ precursors: (a) $LiCu_{0.025}Mn_{1.975}O_4$, (b) $LiCu_{0.05}Mn_{1.95}O_4$, and (c) $LiCu_{0.10}Mn_{1.975}O_4$.

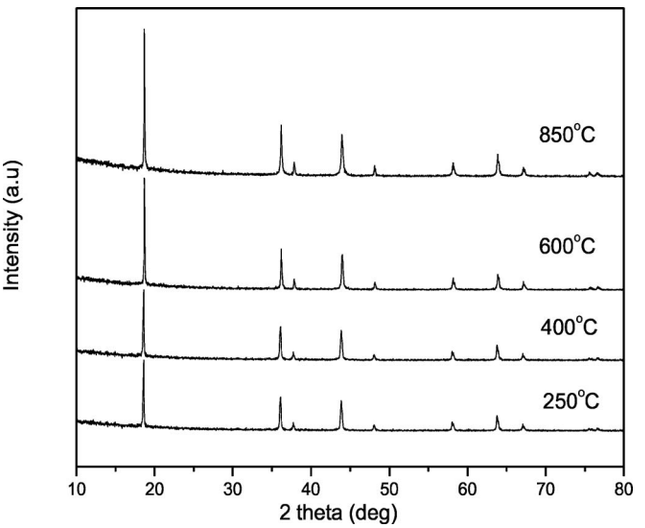

Figure 3. XRD patterns of $LiCu_{0.1}Mn_{1.99}O_4$ calcined at different temperatures: (a) 250, (b) 400, (c) 600, and (d) 850°C.

Results and Discussion

Thermal studies.— Figures 2a-c present TG/DTA curves of $LiCu_xMn_{2-x}O_4$ precursors with different Cu doping levels. The thermal behavior of TG/DTA plots (Fig. 2a and b) for the precursors with Cu levels of $x = 0.025$ and 0.05 show a similar trend. These curves exhibit two exothermic peaks centered at around 150 and 250°C. The first exothermic event corresponding to a weight loss of 22% may be ascribed to the removal of water. The second exothermic peak is combined with a huge weight loss of 40% over a temperature range of 200–330°C and assigned to the formation of the respective oxides. Gravimetrically stable behavior observed beyond 300°C confirms the completion of thermal events. Furthermore, it is apparent that the sol-gel synthesis using oxalic acid as the chelating agent with the respective metal salts proceeds via oxalate intermediates, resulting in the formation of spinel compound. This fact is supplemented by FTIR spectra of the precursors (Fig. 4d). Even though the profile of TG curves for these precursors are similar in all the cases, an overall reduction in weight loss (only 40% as against 62%) is observed in the case of precursor with higher Cu dopant level (Fig. 2c). Furthermore, it is also interesting to note that the DTA plot for the precursor with higher Cu dopant level is quite different. Although the thermal events appear around 100–330°C in all the cases, the first exothermic zone is accomplished with two peak signatures centering between 105 and 150°C in the case of samples with 0.1 Cu. This may be ascribed to the earlier progression of the thermal decomposition reaction of the slightly excess copper nitrates. Furthermore, the reduction in overall weight loss may be due to the complete decomposition of oxalate intermediates. Thus, the thermal analysis data ratifies that the formation of copper-doped spinel begins above 250°C, as is evident from the appearance of a low-intensity peak signature in the XRD pattern at 250°C (Fig. 3) corresponding to plane 111 at ~19° 2θ angle.

X-ray diffraction.— Figure 3 shows the XRD patterns of $LiCu_{0.10}Mn_{1.90}O_4$ calcined at 250, 400, 600, and 850°C. The diffraction profiles match well in accordance with the JCPDS card no. 35-782 confirming the formation of pristine spinel product without any impurity even calcined at 250°C. The appearance of narrow peaks with comparable width in the XRD patterns at all temperatures indicates that the samples possess high crystallinity. The XRD profile of the sol-gel-derived $LiCu_{0.1}Mn_{1.99}O_4$ is in good agreement with that of $LiCu_{0.1}Mn_{1.99}O_4$[21] synthesized through the solid-state technique. The XRD pattern for the sample heated at 850°C shows high-intensity peaks corresponding to planes (111), (311), and (400), thereby confirming the occupancy of lithium ions in tetrahedral 8a sites, and the manganese ions in 16d sites and O^{2-} ions in 32e sites.[22] The small peaks corresponding to planes (533) and (622) indicate the occupancy of a small amount of copper in 8a tetrahedral sites in the spinel structure.

FTIR spectroscopy.— Figure 4d depicts a typical FTIR profile for $LiCu_{0.025}Mn_{1.975}O_4$ and $LiCu_{0.1}Mn_{1.99}O_4$ precursors. The bands centered between 1416 and 1574 cm^{-1} indicate that the process of spinel formation takes place through oxalate intermediates. The

Downloaded 13 Feb 2009 to 210.212.252.226. Redistribution subject to ECS license or copyright; see http://www.ecsdl.org/terms_use.jsp

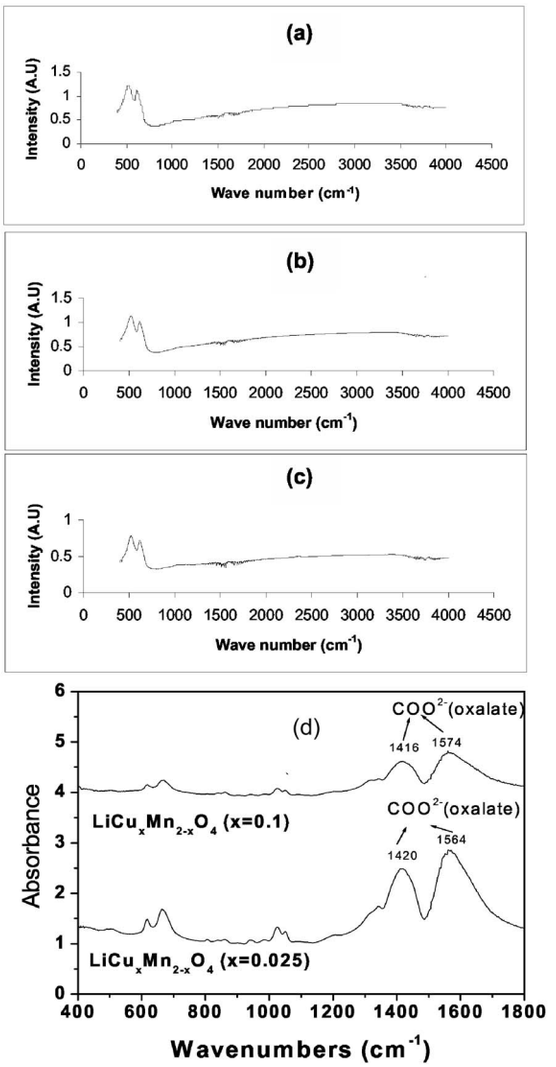

Figure 4. FTIR spectra of different dopant levels of $LiCu_xMn_{2-x}O_4$ calcined at 850°C: (a) 0.025, (b) 0.05, and (c) 0.10. (d) FTIR spectra of $LiCu_xMn_{2-x}O_4$ precursors.

FTIR spectra of $LiCu_xMn_{2-x}O_4$ at various copper doping levels (viz. 0.025, 0.05, and 0.10) calcined at 850°C are shown in Fig. 4a-c. The adsorption peaks for Mn–O and Cu–O are seen around 521.26 and 614.98 cm^{-1}, respectively. These bands are ascribed to the stretching vibration of Mn–O and Cu–O bond.[23-25] A slight shift in absorption peaks (519.86 and 615.78 cm^{-1}) for Mn–O and Cu–O are observed at higher copper dopant levels (x = 0.05 and 0.10). Furthermore, the absence of oxalate peaks at higher wavenumber may be ascribed due to the complete decomposition of nitrate precursors. This vindicates that the precursors were completely decomposed and resulted in the formation of a pristine spinel compound.

SEM and TEM analysis.— Figures 5a-c show the SEM images of $LiCu_xMn_{2-x}O_4$ at different copper doping levels (viz. 0.025, 0.05, and 0.10) calcined at 850°C. It is evident from Fig. 5a-c that the copper-doped spinel particles are of submicrometer-sized spherical-shaped grains. A typical TEM image and diffraction pattern of the $LiCu_{0.1}Mn_{1.99}O_4$ sample is shown in Fig. 5d. It is evident that the particles are very crystalline and present as agglomerates, with average grain size of the primary particles are ~50 nm.

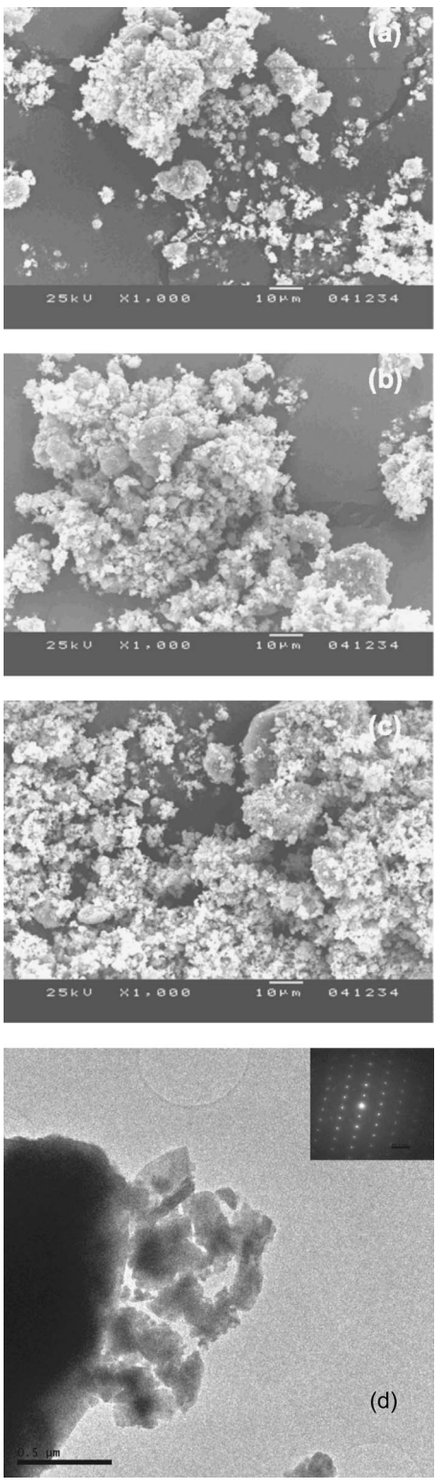

Figure 5. SEM images of different dopant levels of $LiCu_xMn_{2-x}O_4$ particles viz., (a) 0.025, (b) 0.05, and (c) 0.10 calcined at 850°C. (d) TEM image of $LiCu_{0.1}Mn_{1.99}O_4$ particles calcined at 850°C.

Charge–discharge studies.— Figures 6-8 depict the charge–discharge and cycling behavior of $LiCu_xMn_{2-x}O_4$ samples with different copper concentrations (viz. 0.025, 0.05, and 0.10) calcined at 850°C, respectively. The cells were cycled between 3.0 and 5.0 V at a C/10 rate. The sample with the low amount of copper (x

Downloaded 13 Feb 2009 to 210.212.252.226. Redistribution subject to ECS license or copyright; see http://www.ecsdl.org/terms_use.jsp

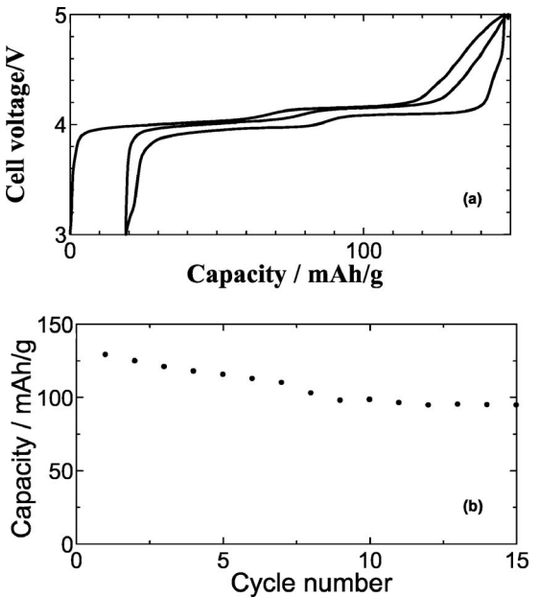

Figure 6. (a) Typical charge–discharge behavior of $LiCu_{0.025}Mn_{1.975}O_4$ calcined at 850°C. (b) Cycle number vs capacity of $LiCu_{0.025}Mn_{1.975}O_4$ calcined at 850°C.

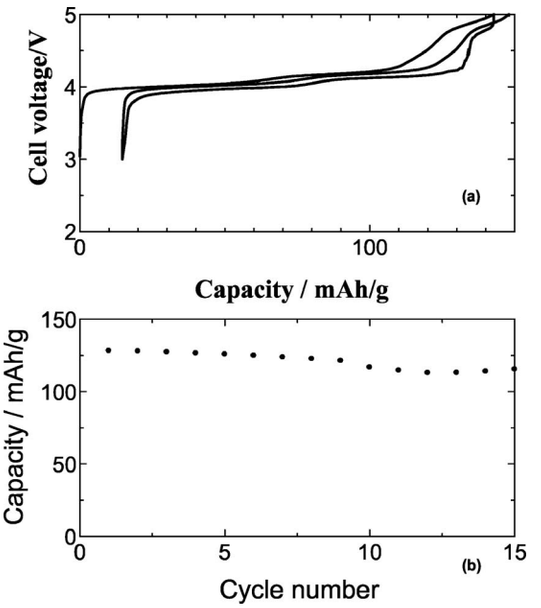

Figure 8. (a) Typical charge–discharge behavior of $LiCu_{0.10}Mn_{1.9}O_4$ calcined at 850°C. (b) Cycle number vs capacity of $LiCu_{0.10}Mn_{1.9}O_4$ calcined at 850°C.

= 0.025) with spinel structure exhibits a specific capacity of 130 mAh g^{-1} during the first discharge. Furthermore, it can be seen that an increase in the initial discharge capacity is observed with an increase in the dopant concentration up to the investigated level of 0.10 Cu. In the case of electrodes with 0.05 Cu, the discharge capacity stabilizes at ~100 mAh g^{-1} and, for those with 0.10 Cu, the discharge capacity stabilizes at ~120 mAh g^{-1} over the investigated 15 cycles. Furthermore, in the present case, it can be seen that, at lower concentration of Cu doping (0.025 and 0.05), two plateaus appear in the 4 V region and, at 1.0 Cu stoichiomentry, the two plateaus in the 4 V region diminish and a new plateau emerges at ~4.9 V, attributed to the Cu^{2+}-to-Cu^{3+} oxidation state. The present results are superior to earlier studies of Ein-Eli et al.,[21] wherein $LiCu_{0.1}Mn_{1.99}O_4$ spinel has been synthesized through the solid-state route with Cu doping (0.1–0.5) delivering an initial discharge capacity of 120 mAh g^{-1} stablizing at 70 mAh g^{-1} after 15 cycles.

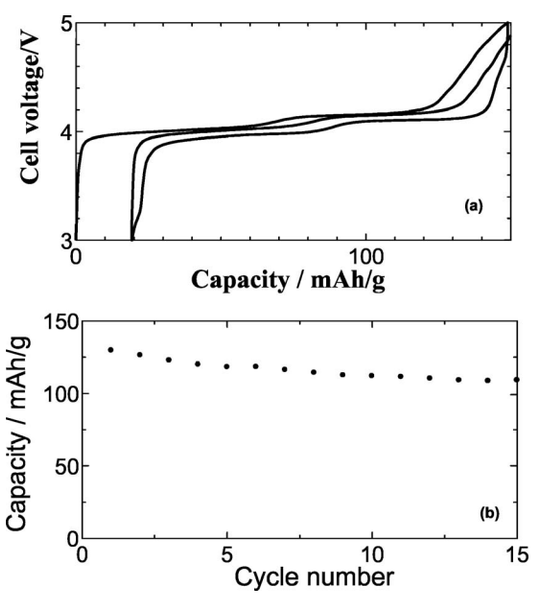

Figure 7. (a) Typical charge–discharge behavior of $LiCu_{0.05}Mn_{1.95}O_4$ calcined at 850°C. (b) Cycle number vs capacity of $LiCu_{0.05}Mn_{1.95}O_4$ calcined at 850°C.

Conclusion

$LiCu_xMn_{2-x}O_4$ (x = 0.025, 0.05, and 0.10) has been synthesized through an oxalic acid–assisted sol-gel route for use as cathode material in lithium rechargeable batteries capable of operating up to 5 V. XRD analysis confirms that this synthesis route yields spinel product even at a low calcination temperature of 250°C. These electrochemically active particles, on the average, are of 50 nm in size and present as agglomerated clusters, which is evident from TEM analysis. The charge–discharge cycling studies on these materials with 0.1 Cu stoichiometry calcined at 850°C exhibit an initial discharge capacity of 130 mAh g^{-1} and stabilized at 120 mAh g^{-1}.

Acknowledgments

The authors thank the Japan Science and Technology Agency, Japan for funding this CREST project.

Central Electrochemical Research Institute assisted in meeting the publication costs of this article.

References

1. T. Ohuzuku, M. Kitagawa, and T. Hirai, *J. Electrochem. Soc.*, **137**, 760 (1990).
2. W. J. Macklin, R. J. Neat, and R. J. Powell, *J. Power Sources*, **34**, 39 (1991).
3. M. Vanev, A. Momchilov, A. Sassalevska, and A. A. Kozawa, *J. Power Sources*, **41**, 305 (1993).
4. D. Guyomard and J. M. Tarascon, *Solid State Ionics*, **69**, 222 (1994).
5. Y. Xia and M. Yoshio, *J. Electrochem. Soc.*, **144**, 2593 (1997).
6. G. Pistoia, A. Antonini, R. Rosati, and D. Zane, *Electrochim. Acta*, **41**, 2863 (1996).
7. G. Kumar, H. Schlorb, and D. Rahner, *Mater. Chem. Phys.*, **70**, 117 (2001).
8. R. J. Gummow, A. Dckock, and M. M. Thackeray, *Solid State Ionics*, **69**, 222 (1994).
9. A. Yamada, *J. Solid State Chem.*, **122**, 100 (1996).
10. S. T. Myung, H. T. Chung, S. Komaba, N. Kumagai, and H. B. Gu, *J. Power Sources*, **90**, 103 (2000).
11. D. H. Jang, J. Y. Sin, and S. M. Oh, *J. Electrochem. Soc.*, **103**, 2204 (1996).
12. Y. Huang, J. Li, and D. Jia, *J. Mater. Sci.*, **41**, 4163 (2006).
13. X.-C. Tang, C.-K. Jiang, C.-Y. Pan, B.-Y. Huang, and Y.-H. He, *J. Solid State Chem.*, **179**, 1100 (2006).

Downloaded 13 Feb 2009 to 210.212.252.226. Redistribution subject to ECS license or copyright; see http://www.ecsdl.org/terms_use.jsp

14. X. M. He, J. J. Li, Y. Cai, C. Y. Jiang, and C. R. Wan, *Mater. Chem. Phys.*, **95**, 105 (2006).
15. A. Caballero, M. Cruz, L. Hernán, M. Melero, J. Morales, and E. Rodríguez Castellón, *J. Power Sources*, **150**, 192 (2005).
16. B. W. Lee, *J. Power Sources*, **109**, 220 (2002).
17. S. R. Sahaya Prabaharan, M. Siluvai Michael, T. Prem Kumar, A. Mani, K. Athinarayanaswamy, and R. Gangadharan, *J. Mater. Chem.*, **5**, 1035 (1995).
18. J. H. Lee, J. K. Hong, D. H. Yang, Y. K. Sun, and S. M. Oh, *J. Power Sources*, **89**, 7 (2000).
19. S. Bach, M. Henry, N. Baffier, and J. J. Livage, *J. Solid State Chem.*, **80**, 325 (1990).
20. J. P. Pereira-Romas, *J. Power Sources*, **54**, 120 (1995).
21. Y. Ein-Eli, W. F. H. Sharan, and H. Lu, *J. Electrochem. Soc.*, **145**, 1238 (1998).
22. M. M. Thackeray, P. J. Johnson, and L. A. Depicciotto, *Mater. Res. Bull.*, **19**, 179 (1984).
23. C. Julien and M. Massot, *Phys. Chem. Chem. Phys.*, **4**, 4226 (2002).
24. E. C. Heltemes, *Phys. Rev.*, **141**, 803 (1966).
25. G. Kliche and Z. V. Popovic., *Phys. Rev. B*, **42**, 10060 (1990).

Downloaded 13 Feb 2009 to 210.212.252.226. Redistribution subject to ECS license or copyright; see http://www.ecsdl.org/terms_use.jsp